FAEQ A. AL-TEMIMEI [1], SHAYMAA AWAD KADHIM [2], NAEEMA HADI ALI [3]

Department of Physics, College of Sciences, University of Kufa
(Al-Najaf, Iraq; ORCID: [1] 0000-0002-3991-5318, [3] 0009-0008-6066-9976;
e-mails: [1] faeqa.jasim@uokufa.edu.iq, [2] shaymaa.alshebly@uokufa.edu.iq,
[3] naemah.abbood@uokufa.edu.iq)

A DFT STUDY OF CENOBAMATE AND ITS NEW ISOMERS AS MEDICATIONS FOR AN EFFECTIVE MEDICAL TREATMENT OF EPILEPSY

UDC 539

Many anti-epileptic drugs use cenobamate, a voltage-gated sodium channel blocker, to the fullest extent. This study investigates the electronic, quantum chemical, and photolytic properties of Cenobamate and its novel designed isomers. The results show that the LUMOs levels are higher than the HOMO energies. The HOMO levels are unpaired and of s-character locally around the chlorine atoms. The reactivity and stability are explained by the frontier molecular energy values and different biochemical descriptors. All isomers have smallest energy gap means with a higher reactivity for biological applications. The most frequent reaction sites are found to be the three acyl carbons in the cenobamate molecule, the chloride related to the phenyl ring, the heterocyclic ring, and the carbonyl oxygen and nitrogen in the ester amide group. The novel isomers have high ability to interact with species, and this takes place either in clinical use or under clinical trials. The isomers are soft compounds, and can easily interact with big soft molecules such as DNA.

Keywords: DFT, B3LYP, cenobamate, isomers, activity.

1. Introduction

Cenobamate, a freshly created drug, is taken orally and is used to treat partial-onset seizures in adults. In November 2019, the US government approved it for the medical use, and in March 2020, Schedule V was added. [(1R)-1-(2-chlorophenyl)-2-(tetrazol-2-yl)ethyl] Cenobamate is chemically known as carbamate, having the molecular formula C10H10ClN5O2. White to off-white crystalline powder known as cenobamate is non-hygroscopic and only tangibly soluble in pure water [1, 2]. Cenobamate has tereoisomerism, because it has a single chiral center. The R-enantiomer of cenobamate is synthesized, and this opens the door for the use of this medication to treat patients with focal seizures that have proven to be resistant to existing treatments [3]. A thorough review of the literature reveals that no research has been published to far that analyze the electrical characteristics of cenobamate [3, 4]. Several research teams have recently used chemical quantum mechanics and density functional theory to study the structure, characteristics, and spectroscopy of medicinal molecules [5–7]. Computational chemists have traditionally found it difficult to conduct quantum chemical analyses of the molecular and predictive features of pharmacologically active substances. In addition, these data are

Citation: AL-Temimei Faeq A., Kadhim Shaymaa Awad, Ali Naeema Hadi. A DFT study of cenobamate and its new isomers as an effective medical treatment for epilepsy medications. *Ukr. J. Phys.* **69**, No. 5, 314 (2024). https://doi.org/10.15407/ujpe69.5.314.

Цитування: Ал-Темімей Фаєк А., Кадхім Шаймаа Авад, Алі Наєєма Хаді. Дослідження на базі теорії функціонала густини властивостей ценобамату і його нових ізомерів як ефективних ліків при епілепсії. *Укр. фіз. журн.* **69**, №5, 314 (2024).

very helpful for understanding how medications interact with physiological target molecules [8, 9]. The quantum mechanical computation can provide data and information on the electronic structures and several compound properties. In addition, it analyzes the crucial information about the electronic structure to be researched and analysed [10]. To obtain significant features such as molecular orbital energy, molecular structures, electronic absorption, and other properties from this method, the density functional theory (DFT) is a trustworthy standard instrument for theoretical processing of structures [9–12]. In this study, it will be interesting to see what happens, when the ligands in the cenobamate drug's with an original chemical structure are replaced by different ligands. The structural, electronic, spectroscopic, and excitation properties of cenobamate were described using the quantum computational approach embodied by density functional theory to ascertain the eventual applicability of these new cenobamate isomers as new active epileptic medications.

2. Computational Details

Utilizing the Lee–Yang–Parr gradient-corrected correlation potential (B3LYP) method with the Gaussian09 package in the ground state at gas phase, as well as Gauss View 5.0.8, which was used to prepare the input files to Gaussian09 and depict the initial structure of the molecules, the geometry optimizations, electronic structure, and energy, the calculations were carried out [13–15]. Using polarized split-valence 6-311G* (d,p) basis sets, all calculations were performed without any symmetry restrictions. Using the same basis sets at the hybrid functional, TD-DFT has been used to calculate the permitted excitations and oscillator strengths for the attributes of exactions state CAM-B3LYP [15, 17].

3. Results and Discussion

3.1. The Structure Properties

Figure 1 depicts the relaxed structure of cenobamate (C1) and its intended derivatives (C2-C6) (isomers) (White atoms are hydrogen; gray atoms are carbons; red ones are oxygens, blue are nitrogens, and green atom are chlorines). The results from the DFT method demonstrated the usefulness of the theory in determining the geometrical optimization of molecular structures, where the optimized structure is at

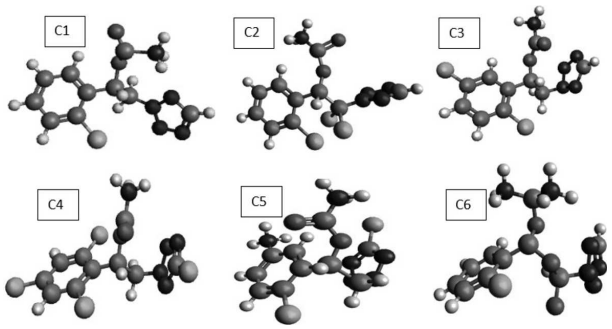

Fig. 1. Denoted the optimized geometry of the Cenobamate and its isomers

the global minimum in the range of the virial ratio "–V/T" from 2.0041 to 2.0033 and the relaxed structure is completed without any imaginary frequency. These findings are due to the fact that the DFT approach incorporates all corrections for electron interactions in the molecular structure, and that the theoretical DFT method is effective at optimizing and improving the geometrical properties of a molecular structure. The intervals of bond lengths for the molecules are: C=C = 1.378– 1.431 Å, C–C = 1.363–1.571 Å, N–C = 1.309–1.311 Å, N=C = 1.337–1.339 Å, N–N = 1.778–1.763 Å, N–H = 1.061–1.072Å, and C–H = 1.068–1.073 Å exhibiting a delocalized π-bond character, and these values are in good agreement with values of the experimental. The link between the aromatic carbon and the chlorine atom bonded to the phenyl ring has the longest length, measuring 1.6615–1.763. The molecules' geometric properties, including their bonds and angles, were in good agreement with the values obtained from X-ray data. For instance, the dihedral angles were between 180° and –180°, the inter-ring bonds were around the value 1.4203, and the C–C–C bonds were about 120° [19, 20].

4. Electronic Properties

The electrical properties of the substances under study are listed in Table 1 (C1–C6). As a result, higher levels of HOMO suggest a better tendency for electron donation, which improves the inhibitor for mild steel's ability to bind to the metal and improves inhibition effectiveness. The ability of a molecule to accept electrons is referred to as "LUMO". The inhibitor molecule's responsiveness to adsorption on the metallic surface is significantly influenced by the energy gap value. Understanding how the HOMO, LUMO, and gap energies explain the properties of

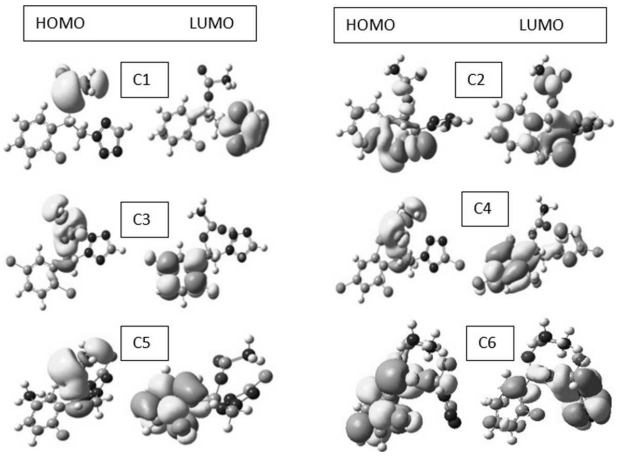

Fig. 2. The plots of Electrostatic Potential on the van der Waals surface for C1–C6 molecules

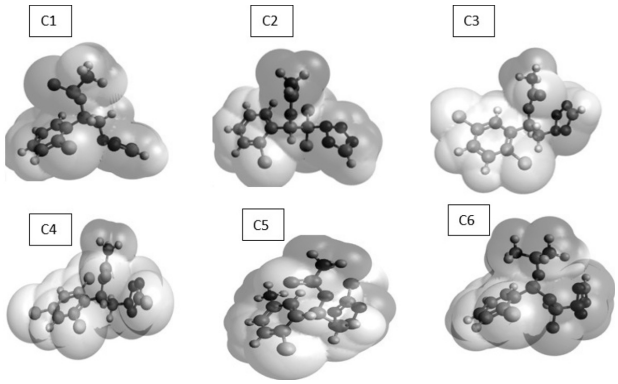

Fig. 3. The plots of Electrostatic Potential on the van der Waals surface for C1–C6 molecules

Table 1. **The electronic properties for the Cenobamate and its isomers (C1–C6)**

Proprieties (eV)	Isomers					
	C1	C2	C3	C4	C5	C6
HOMO Energy	–9.031	–6.502	–6.631	–6.930	–7.167	–7.810
LUMO Energy	0.570	–2.859	–4.272	–4.353	–4.435	–4.506
Energy gab	9.601	3.643	2.359	2.577	2.732	3.304
Ionization potential	9.031	6.502	6.631	6.930	7.167	7.810
Electron affinity	–0.570	2.859	4.272	4.353	4.435	4.506
Chemical potential	4.230	4.681	5.451	5.641	5.801	6.158
Global hardness	4.801	1.821	1.180	1.288	1.366	1.652
Global softness	0.104	0.275	0.424	0.388	0.366	0.303
Electronegativity	–4.230	–4.681	–5.451	–5.641	–5.801	6.158
Electrophilicity index	1.864	6.014	12.597	12.351	12.318	11.478

the chemical stability of molecules is essential in order to calculate the energy of the transmitted electron. The stability of the compound, chemical reactivity, and optical and electrical properties are all governed by energy. The smaller energy gap is an indicator of the compound's biological reactivity. The cenobamate is an insulator with a large energy gap [21]. The new isomers under study have been used in the semiconductor industry. As a result, it must be related to the lower optical energy transmission in the electronic spectrum. The greater the reactivity for biological applications, the smaller the value of the gap. Effectiveness in the order of the molecules should be: C3 > C4 > C5 > C6 > C2 > C1, according to the energy gap values.

Chemical descriptors are crucial, because they forecast the compound's biological function. Therefore, it is obvious that the newly created isomers are more successful in the disease treatment based on the calculations of the electronic properties provided in Table 1, which is a summary of the results. The novel isomers are reactive and can interact with the biomolecules if used as medicine, which is supported by the drug's application in both sterilizing and disease therapy. The biological action of the medicine is also significantly influenced by the chemical structure and the addition of new ligands. Each molecule's coordination determines, Fig. 2 shows the distribution of the border molecular orbital (HOMOs and LUMOs) features of cenobamate and its isomers in 3-D due to the LCAOs-MOs. The HOMO is found in the ester amide ring of cenobamate, the nitrogen atoms, the carbonyl oxygen, the ether oxygen, the heterocyclic ring, the phenyl ring, the chlorine atom connected to the phenyl ring, and so on. LUMO is present in both the phenyl and heterocyclic rings of cenobamate, in contrast. Chemical descriptors are important, because they can be used to predict the biological function of a molecule.

5. Electrostatic Potential

The non-covalent interaction between polarized structures is significantly influenced by the electrostatic potential, which also explains the electrophilic or nucleophilic behavior by controlling the interaction area and strength of the electrostatic and inductive forces. It is crucial to remember that the entire charge distribution surrounding a molecule is what causes ESP. The van der Waals surface map coloured by ESP

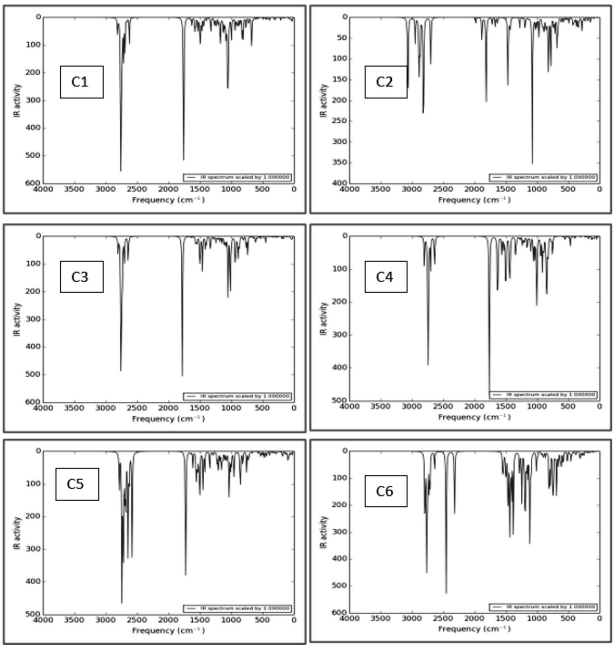

Fig. 4. IR-Spectra of the all compounds under study

of Fig. 3 depicts all of the compounds under consideration and shows how the potentials were drawn toward the areas of high electronegativity. This helps the viewer to understand how to identify the positions of each compound's actual ends in relation to the species around them. However, the positive diffusion region and the negative diffusion region, respectively, are represented by the colours red and blue. Moreover, color coding is utilized to depict the various electrostatic potential values; high ESP values are shown in blue, low ESP values are shown in red, and the region of zero potential is shown in white.

6. Infrared IR Spectra

Figure 4 displays the examined compounds' infrared IR spectra as determined by B3LYP/DFT at 6-311G* (d,p) level calculations. The spectra for compound C1 revealed that the C–H bonds were stretched at (3027.74–3239.42) cm^{-1} corresponding to low intensities equal to 49.891 km/mol and 0.111 Km/mol, respectively. The stretching C–C bonds lie at (1546.73–1675.25) cm^{-1} with maximum intensity to be 70.596 Km/mol corresponding to 1617.64 cm^{-1}. The stretching C–O bond is seen at 1270.54 cm, while the bending C–H bonds are seen at (1411.081–1530.232) cm^{-1}. Moreover, the C–Cl bond's stretching is noticed at (861.45–8711.101) cm^{-1}. For compounds C2–C6, the stretching C–H bonds lie in the interval (3036.64–3242.26) cm^{-1} with maximum intensity equaled to 122.67–132.75 Km/mol. These computed values are consistent with experimentally measured values for phenyl compounds [12]. The stretching C–N bonds are observed at 2263.42–2322.34 cm^{-1} corresponding to 71.174–73.543 Km/mol intensity. The bending C–H bonds are observed at (1481.46–1528.36) cm^{-1} while the stretching C–O was observed at 1282.78 cm^{-1} corresponding to high intensity 491.165 Km/mol. Figure provides the illustration of the additional vibration modes for the compounds in this study. Results from the experiment for cyclic carbon compounds are consistent with the above findings [22].

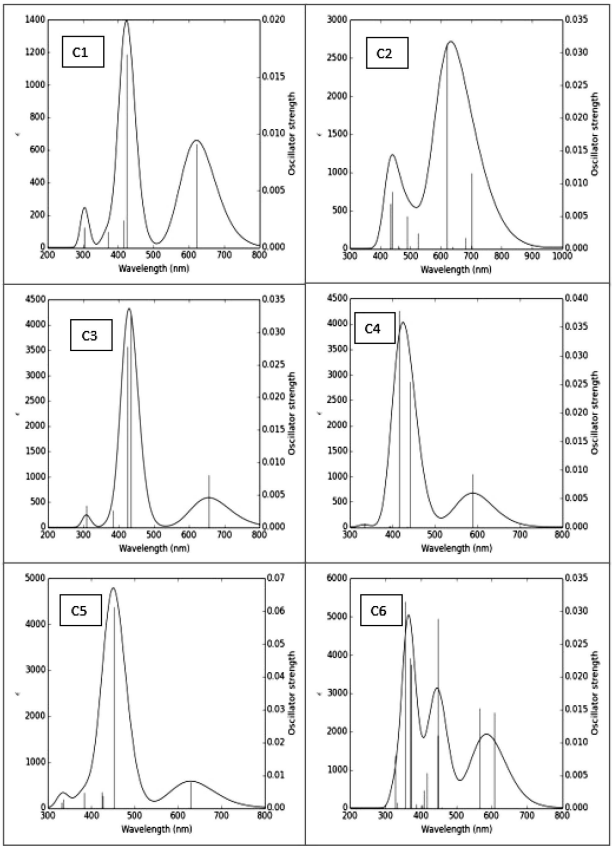

Fig. 5. Illustrates the simulated UV-visible spectrum of the Cenobamate and its isomers

7. Electronic Spectra

Electronic transitions and, by extension, electronic spectra, are time-dependent processes that can be modeled by TD-DFT simulations. To determine whe-

Table 2. **The electronic spectra properties of Cenobamate and its isomers under study**

Isomers	State	$E_{ex.}$ (eV)	λ_{max} (nm)	Transition types	Major Transition (H = HOMO, L = LUMO)
C1	S1	1.9949	621.49	$n \to \pi^*$	H−1(B) → L+1(B), H−1(B) → L+3(B), H (B) → L+1(B), H (B) → L+2(B), H−1 (A) → L+2(A)
	S2	2.9209	424.48	$n \to \pi^*$	H−1 (A) → L (A), H−6(A) → L (A), H−5(A) → L+4(A), H−3(A) → L (A), H−1 (B) → L+1 (B), H−3(B) → L (B)
	S3	3.5566	348.60	$\pi \to \pi^*$	H (A) → L+2(A), H (A) → L+3(A), H (A) → L+1 (A), H (B) → L+5(B), H−1(B) → L+2 (B)
C2	S1	1.8205	621.49	$n \to \pi^*$	H (A) → L (A), H (A) → L+1(A), H (A) → L+2(A), H (A) → L+5(A), H (A) → L+6(A), H(B) → L+2(B), H (B) → L+7(B)
	S2	2.6954	459.99	$n \to \pi^*$	H (A) → L (A), H−2(A) → L (A), H−4(A) → L+4(A), H−3(A) → L (A), H−1 (B) → L+2 (B), H−2(B) → L+1 (B)
C3	S1	1.8913	655.54	$n \to \pi^*$	H−2 (A) → L (A), H−3(A) → L+1 (A), H−4(A) → L+1(A), H−5(A) → L (A), H−2 (B) → L+1 (B), H−2(B) → L+3 (B)
	S2	2.8047	442.06	$n \to \pi^*$	H (A) → L+1(A), H (A) → L+2(A), H−2 (A) → L+1 (A), H (B) → L+4(B), H−1(B) → L+1 (B)
	S3	3.6124	343.22	$\pi \to \pi^*$	H (A) → L (A), H (A) → L+1(A), H (A)→L+1(A), H (A) → L+3(A), H (A)→L+6(A), H(B) → L+1(B)
C4	S1	2.0649	600.43	$n \to \pi^*$	H (A) → L (A), H−3(A) → L (A), H−3(A) → L+1(A), H−3(A) → L (A), H−2 (B) → L+4 (B), H−4(B) → L+1 (B)
	S2	2.8130	440.76	$n \to \pi^*$	H−2(B) → L (B), H−1 (B) → L+1(B), H (B) → L+3(B), H−1 (A) → L (A)
C5	S1	1.9715	655.54	$n \to \pi^*$	H−1 (A) → L+1(A), H (A) → L+1(A), H (A) → L+3(A), H (A) → L+4(A), H−1(B) → L+2(B), H (B) → L+2(B)
	S2	2.7393	452.62	$n \to \pi^*$	H−1 (A) → L (A), H (A) → L+1(A), H (A) → L+2(A), H (A) → L+3(A), H(B) → L+2(B), H (B) → L+2(B)
	S3	3.6333	341.25	$\pi \to \pi^*$	H−1 (A) → L (A), H−2(A) → L+1 (A), H−1 (A) → L+2(A), H−1(A) → L+3 (A), H−2 (B) → L+4 (B), H−4(B) → L+1 (B)
C6	S1	3.6333	341.25	$n \to \pi^*$	H−2 (A) → L+2(A), H−1 (A) → L+1(A), H (A) → L+1 (A), H (B) → L+2(B), H−1(B) → L+2 (B)
	S2	2.7049	458.36	$n \to \pi^*$	H−2 (A) → L (A), H−2(A) → L+2 (A), H−3(A) → L+4(A), H−3(A) → L (A), H−3 (B) → L+2 (B), H−2(B) → L+1 (B)
	S3	2.7049	458.36	$\pi \to \pi^*$	H (A) → L+1 (A), H−1(A) → L (A), H−2(A) → L+3(A), H−3(A) → L (A), H−1 (B) → L+2 (B), H−1(B) → L+2 (B)

ther the electronic transitions were time-dependent phenomena, TD-DFT simulations with the hybrid functional CAM-B3LYP and 6-311G* (d,p) basis set were performed in this work using GaussSum [23, 24]. The frontier orbitals (HOMOs and LUMOs), which are important in electronic spectra and chemical processes, play a crucial role. The energy gap of the cenobamate and its isomers, which include unpaired electrons, is between (2.359–3.643) eV. This interval of energy gaps corresponds to the UV-vis region of electromagnetic radiation, as shown in Fig. 5. Table 2 lists the main band, transition types, and key transition excitation energies (from HOMO to LUMO).

8. Conclusions

This study has explored the optimized structure of the pharmacologically active cenobamate and its novel isomers. The geometrical parameters values of cenobamate and its isomers are in a good agreement with experimental data, this indicates to a good relax was obtained from the suitable functional and basis sets. The LUMOs are greater than the HOMOs, and they are distributed according to LCAO, Being the HOMO level unpaired and of s-character locally around the chlorine atoms. The reactivity and stability are explained by the frontier molecular energy values and different biochemical descriptors. All isomer have smallest energy gaps with the higher reactivity for biological applications. The acyl carbons in the cenobamate molecule, the chloride connected to the phenyl ring, the heterocyclic ring, and the carbonyl oxygen and nitrogen in the ester amide group are determined to be the most prevalent reaction sites. The novel isomers have high ability to interact with species, and it takes place either in clinical use or under clinical trials. The isomers are soft compounds, they can easily interaction with big soft molecules such as DNA.

1. R. Roberti, C. De Caro, L.F. Iannone *et al.* Pharmacology of cenobamate: Mechanism of action, pharmacokinetics, drug-drug interactions and tolerability. *CNS Drugs* **35**, 609 (2021).
2. N. Das, M. Dhanawat, S.K. Shrivastava. An overview on antiepileptic drugs. *Drug Discov Ther.* **6**, 178-93 (2012).
3. S.S. Chung, J.A. French, J. Kowalski *et al.* Randomized phase 2 study of adjunctive cenobamate in patients with uncontrolled focal seizures. *Neurology* **94**, e2311 (2020).
4. J.A. French. Cenobamate for focal seizures – a game changer? *Nat. Rev. Neurol* **16**, 4 (2020).
5. F.A. Mohammed, H.I. Abbood. Electronic structure of vanadium tetrachloride di-hydroxyl metal complex. *J. Engin. Appl. Sci.* **13**, 9823 (2018).
6. K. Bamba, O.W. Patrice, N. Ziao. NBO Population analysis and electronic calculation of four azopyridine ruthenium complexes by DFT method. *Comput. Chem.* **5**, 51 (2017).
7. A.A. Muhmood, F.A. AL-Temimei. New ruthenium metal complexes for their activity with DNA and cells of cncer/DFT-B3LYP calculations. *Indian J. Public Health* **10**, 1241 (2019).
8. A.F. LeRoy. Interactions of platinum metals and their complexes in biological systems. *Environmental Health Perspectives* **10**, 73 (1975).
9. A.S. Abu-Surrah, M. Kettunen. Platinum group antitumor chemistry: Design and development of new anticancer drugs complementary to cisplatin. *Current Med. Chem.* **13**, 1337 (2006).
10. K. Zheng, J. Wang, Y. Shen *et al.* Studies on 4,7-di-substitution effects of one ligand in $[Ru(Phen)_3]^2$ with DFT method. *J. Comput. Chem.* **23**, 436 (2002).
11. J. Foresman, E. Frish. *Exploring chemistry.* (Gaussian Inc., 1996).
12. P. Hohenberg, W. Kohn. Inhomogeneous electron gas. *Phys. Rev.* **136**, b864 (1964).
13. M.J. Frisch, G.W. Trucks, H.B. Schlegel *et al. GAUSSIAN 09, Revision A.02.* (Gaussian, Inc., CT, 2009).
14. P.J. Hay, W.R. Wadt. Ab initio effective core potentials for molecular calculations – potentials for the transition-metal atoms Sc to Hg. *J. Chem. Phys.* **82**, 270 (1985).
15. F.A. AL-Temimei, H.A. Mraity. DFT/TD-DFT investigation of novel D-π-A configuration dyes for improving solar cell efficiency. *Struct Chem.* **33**, 859 (2022).
16. J.B. Collins, P.V. Schleyer, J.S. Binkley *et al.* Self-consistent molecular orbital methods. XVII. Geometries and binding energies of second-row molecules. A comparison of three basis sets. *J. Chem. Phys.* **64**, 5142 (1976).
17. F.A. AL-Temimei. Design high-efficiency organic dyes based on fluorescein toward dye-sensitized solar cells: A DFT/TD-DFT study. *Opt Quant Electron* **54**, 600 (2022).
18. A Kumar, V. Deval, P. Tandon, A. Gupta. Experimental and theoretical (FT-IR, FT-Raman, UV-Vis, NMR) spectroscopic analysis and first-order hyperpolarizability studies of non-linear optical material: (2E)-3-[4-(methylsulfanyl) phenyl]-1-(4-nitrophenyl) prop-2-en-1-one using density functional theory. *Spectrochimica Acta Part A.* **130**, 41 (2014).
19. R.T. Morrison, R.N. Boyd. *Organic Chemistry* (New York University, 2007).
20. W.B. De Almeida, H.F.D Santos, P.J. O'Malley. A molecular mechanics and semiempirical conformational analysis of the herbicide diuron inhibitor of photosystem II. *Struct Chem.* **6**, 383 (1995).
21. T. Pooventhiran, U. Bhattacharyya, D.J. Rao *et al.* Detailed spectra, electronic properties, qualitative non-covalent interaction analysis, solvatochromism, docking and

molecular dynamics simulations in different solvent atmosphere of cenobamate. *Struct Chem.* **31**, 2475 (2020).
22. P. Atkins, R. Friedman, *Molecular Quantum Mechanics* (Oxford University Press Inc, 2005).
23. M.E. Casida, C. Jamorski, K.C. Casida *et al.* Molecular excitation energies to high-lying bound states from time-dependent density-functional response theory: Characterization and correction of the time-dependent local density approximation ionization threshold. *J. Chem. Phys.* **108**, 4439 (1998).
24. R. Bauernschmitt, R. Ahlrichs. Treatment of electronic excitations within the adiabatic approximation of time dependent density functional theory, *Chem. Phys. Lett.* **256**, 454 (1996).

Received 08.05.23

Фаєк А. Ал-Темімей,
Шаймаа Авад Кадхім, Наєема Хаді Алі

ДОСЛІДЖЕННЯ НА БАЗІ ТЕОРІЇ ФУНКЦІОНАЛА ГУСТИНИ ВЛАСТИВОСТЕЙ ЦЕНОБАМАТУ І ЙОГО НОВИХ ІЗОМЕРІВ ЯК ЕФЕКТИВНИХ ЛІКІВ ПРИ ЕПІЛЕПСІЇ

Вивчаються електронні, квантовохімічні і фотолітичні властивості ценобамату, який блокує натрієві канали, та його нових ізомерів. Знайдено, що центрами з найбільшою реакційною здатністю є три атоми вуглецю в ценобаматі, хлорид фенільного кільця, а також кисень карбонільної групи і атом азоту в амідній групі.

Ключові слова: теорія функціоналу густини, B3LYP, ценобамат, ізомери, активність.